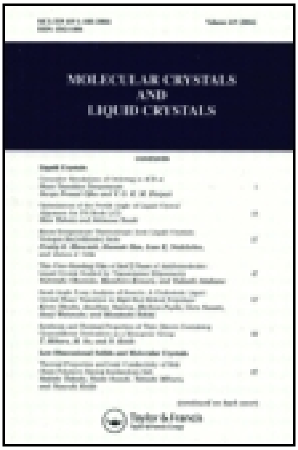

Molecular Crystals and Liquid Crystals

Publication details, including instructions for authors and subscription information:
http://www.tandfonline.com/loi/gmcl20

MOLECULAR DYNAMICS SIMULATION OF AN ANTIFERROELECTRIC LIQUID CRYSTALLINE MOLECULE MHPOBC: CONFORMATIONAL TRANSITION IN SMECTIC PHASES

Hirokazu Toriumi [a], Masafumi Yoshida [b], Nozomu Kamiya [c] & Munetaka Takeuchi [c]

[a] Department of Chemistry, Graduate School of Arts and Sciences, The University of Tokyo, 3-8-1 Komaba, Meguro-ku, Tokyo 153-8902, Japan

[b] Musashi Institute of Technology, 1-28-1 Tamazutsumi, Setagaya-ku, Tokyo 158-8557, Japan

[c] Life Science & Material Science Division, Fujitsu Ltd., 1-9-3 Nakase, Mihama-ku, Chiba-shi, Chiba 261-8588, Japan

Version of record first published: 15 Jul 2010

To cite this article: Hirokazu Toriumi, Masafumi Yoshida, Nozomu Kamiya & Munetaka Takeuchi (2003): MOLECULAR DYNAMICS SIMULATION OF AN ANTIFERROELECTRIC LIQUID CRYSTALLINE MOLECULE MHPOBC: CONFORMATIONAL TRANSITION IN SMECTIC PHASES, Molecular Crystals and Liquid Crystals, 402:1, 31-42

To link to this article: http://dx.doi.org/10.1080/744816674

Mol. Cryst. Liq. Cryst., Vol. 402, pp. 31/[267]–42/[278], 2003
Copyright © Taylor & Francis Inc.
ISSN: 1542-1406 print/1563-5287 online
DOI: 10.1080/15421400390268546

MOLECULAR DYNAMICS SIMULATION OF AN ANTIFERROELECTRIC LIQUID CRYSTALLINE MOLECULE MHPOBC: CONFORMATIONAL TRANSITION IN SMECTIC PHASES

Hirokazu Toriumi
Department of Chemistry, Graduate School of Arts and Sciences, The University of Tokyo, 3-8-1 Komaba, Meguro-ku, Tokyo 153-8902, Japan

Masafumi Yoshida
Musashi Institute of Technology, 1-28-1 Tamazutsumi, Setagaya-ku, Tokyo 158-8557, Japan

Nozomu Kamiya and Munetaka Takeuchi
Life Science & Material Science Division, Fujitsu Ltd., 1-9-3 Nakase, Mihama-ku, Chiba-shi, Chiba 261-8588, Japan

Molecular dynamics (MD) simulation was carried out for an antiferroelectric liquid crystalline molecule, (S)-4-[(1-methylheptyloxycarbonyl]phenyl 4′-octyloxybiphenyl-4′-carboxylate (MHPOBC), to analyze its conformational property in smectic liquid crystalline phases. The MD simulation reproduces a "solid–SmC_x–SmA–isotropic" phase transition. The MHPOBC molecules in the SmC_x phase are packed in a tilted layered structure, while in the SmA phase the molecular tilt disappears. The chiral alkyl chain in the crystalline phase has a larger gauche population at the C-C bond, which gives rise to a "highly bent structure". In smectic phases, the conformation of both chiral and achiral alkyl chains is almost fully liberated, and the average molecular shape changes into a "moderately bent structure". Comparison of the results of MD simulation and molecular orbital calculation indicates that the smectic phases of MHPOBC can be distinguished from the solid phase in terms of the alkyl chain conformation, and the SmC_x and SmA phases are distinguished from each other in terms of molecular packing structure.*

Keywords: antiferroelectric liquid crystals; conformation; MHPOBC; molecular dynamics simulation; molecular orbital calculation

INTRODUCTION

MHPOBC ((*S*)-4-[(1-methylheptyloxy)carbonyl]phenyl 4′-octyloxy-biphenyl-4′-carboxylate) in Figure. 1, consisting of a biphenyl phenyl ester mesogen core (Core A) to which an achiral alkyl chain (Chain X) and a chiral alkyl chain (Chain Y) are attached, has been extensively studied as the first example of antiferroelectric liquid crystalline molecule [1]. Among them, a single-crystal X-ray study performed by Hori and Endo [2] is quite interesting since it reveals that the MHPOBC molecule in the crystalline phase adopts a peculiar bent conformation, where the chiral alkyl chain is oriented nearly perpendicular to the core moiety. The result of conformation analysis we have carried out in a previous study [3] shows that this "highly bent conformation", which is not the energetically most stable conformation but is the second favored structure, is chosen in the crystalline phase because of asymmetric intermolecular packing constraints. In fact, such anomalous bent structure has not been observed for achiral analogues of MHPOBC, ***e.g.***, 8O-O8 with normal alkoxy chain ($Y = -OC_8H_{17}$) and 8O-8 with normal alkyl chain ($Y = -C_8H_{17}$) [4,5].

Molecular conformation of MHPOBC in liquid crystalline phases, however, has not yet been clearly elucidated. This is mainly due to experimental difficulty in obtaining site-dependent conformational information. Recently, ^{13}C-NMR [6], ^{2}H-NMR [7] and polarized spectroscopy [8] studies have been carried out, and they have shown that the direction of orientation of the chiral chain deviates from the molecular long axis by approximately 42–43° in the SmA phase [6,7]. This result is quite different from the observation of single-crystal X-ray study (which gives a value of 85°) and therefore suggests that the MHPOBC molecule undergoes a conformational melting during the solid – SmC_x – SmA phase transition.

In this study, we have carried out molecular dynamics (MD) simulation of MHPOBC in smectic phases as an extension of our previous solid-state

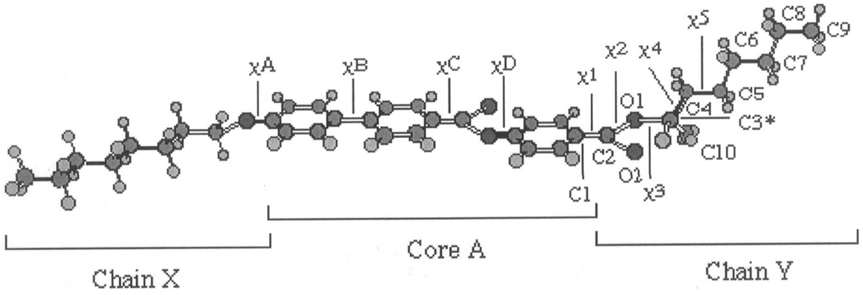

FIGURE 1 Structure of MHPOBC and assignment of torsion angles and backbone atom numbers in the chiral alkyl chain.

simulation and found that the conformational melting does in fact occur when the solid MHPOBC melts into smectic phases. This analysis shows that the MHPOBC molecule in the SmA phase has a "fluid-like" conformation and the average tilt angle of the chiral chain relative to the core moiety has a value of 46° in agreement with the aforementioned NMR observations. In the following, we report the results of MD simulation together with those of molecular orbital (MO) calculations, and present visual illustrations of the molecular conformation and packing structure of MHPOBC in smectic phases.

CALCULATION

(1) Geometry of the Molecule

The fundamental conformational property of MHPOBC has been discussed in our previous papers based on the results of semi-empirical MO calculations [3,5].

The mesogen core (A in Fig. 1) is regarded as a rigid rodlike body: the *para*-axes of the three phenyl groups are aligned linearly. The torsion angle χB between the two phenyl rings in the biphenyl group is found to be centered at 10°, but its distribution varies widely depending on temperature from $\chi B = -10° \sim 30°$ at 400 K to $\chi B = -30° \sim 50°$ at 750 K. The ester group (bridging the biphenyl and phenyl groups) is in the same plane of the biphenyl group ($\chi C = 0°$ or 180°). The rightmost phenyl group in Core A is twisted by more than 60° with respect to the biphenyl group (the χD value may vary in the range of $60° \sim 120°$). The ether linkage group in the octyloxy chain (X in Fig. 1) is oriented in the same plane of the adjacent phenyl group ($\chi A = 0°$, 180°) because of the resonance stabilization effect. The presence of the octyloxy chain has been shown, by both semi-empirical MO and more precise *ab-initio* calculations, to have no significant influences to the conformation of the chiral alkyl chain located at the opposite side of the mesogen core (and vice versa).

(2) MO Calculation

In this study, we focus our attention to the conformational property of the chiral alkyl chain. We therefore carry out our MO calculation for a small fragment (C_6H_5-COO-$CHCH_3C_6H_{13}$) composed of the chiral chain Y and its adjacent phenyl group (as stated above, the chiral chain (Y) conformation is not influenced by the presence or absence of the achiral octyloxy chain (X)). The conformational energy, heat of formation in the MOPAC output, was calculated by using MOPAC6 program and PM3 parameters [9] on a SGI IRIS workstation. This calculation was carried out for more than 8×10^6

conformers with varying the torsion angles χ1–χ5 at every 15° intervals, while maintaining the torsion angles χ6–χ8 at the all *trans* position according to the X-ray observation. All the bond lengths and bond angles are fixed to the standard values [10].

(3) MD Simulation

MD simulation was carried out for a system of 64 MHPOBC molecules under a periodic boundary condition using Fujitsu MASPHYC program on a Fujitsu VP2600/10 UPX vector computer. The simulation was performed in a constant NTP ensemble at 298 K, 400 K, 450 K and 750 K; the temperature T was controlled by the Nose algorithm [11] and the pressure P was kept at 1 atm by the Parrinello and Rahman algorithm [12]. The initial configuration of the system was taken from the X-ray data of crystalline phase [2], and the simulation was performed up to 200 ps with a time step of 0.5 fs. The DREIDING [13] and OPLS [14] force parameters were employed for bonding and non-bonding interactions, respectively. The united atom approximation was employed for CH, CH_2, and CH_3 groups. The electrostatic interactions were calculated by the Ewald method [15] using the electric charges optimized by MO calculation (MOPAC6, PM3, ESP) for the most stable conformations.

RESULTS AND DISCUSSION

(1) MO Calculation

In Figure 2, the results of MO calculations reported in ref 3 are reproduced to aid the discussion. The χ2 rotamer distribution curve shows a symmetric

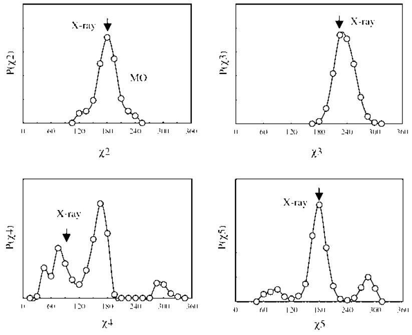

FIGURE 2 Rotamer distribution curves for the χ2–χ5 bonds at 298 K calculated by molecular orbital method (MOPAC6, PM3). Arrows indicate the torsion angles observed in X-ray analysis.

distribution around 180° (the asymmetric carbon atom C3* lies in the ester plane). The effect of introduction of the α-methyl group appears most distinctly in the $\chi 3$ and $\chi 4$ rotamer distribution curves. The torsion angle $\chi 3$ (C2-O1-C3*-C4) has an asymmetrical distribution centered at about 225°, *i.e.*, both the C4 (alkyl) and C10 (methyl) groups are located at the most remote position from the ester C2(O2) group. The $\chi 4$ (O1-C3*-C4-C5) rotamer distribution curve shows a complicated asymmetric shape, since the *gauche* conformation at $\chi 4 = 300°$ is destabilized because of the steric hindrance between C10 (methyl) and C5 (methylene) groups. The rotamer distribution curve for the C5–C6 bond ($\chi 5$) has three major peaks (one *trans* and two *gauche* conformations) characteristic of the alkyl C–C bond. The chiral steric constraints imposed by the -methyl group is thus found to have no significant influences to the rotational states of the $\chi 5$ bond and beyond.

Shown also in Figure 2 are the experimentally observed χi (i = 2–5) rotamer positions taken from the single-crystal X-ray data [2]. They, except the one at $\chi 4$, agree quite well with the calculated peak positions. The result for $\chi 4$, where the X-ray result falls on the *gauche* position ($\chi 4 = 75°$) rather than the energetically favored *trans* position ($\chi 4 = 165°$), indicates that the second stable *gauche* conformation is chosen in the crystalline phase because of intermolecular packing effects.

Figure 3 illustrates the structure of the energetically most favorable *trans* ($\chi 4 = 165°$) conformer and the second stable *gauche* ($\chi 4 = 75°$) conformer (for simplicity the alkyl C–C torsion angles, except that at $\chi 4$ of the chiral chain, are fixed to the *trans*positions according to the X-ray results). The $\chi 4 =$ *gauche* conformer gives rise to a "highly bent" structure which corresponds to the X-ray observation. On the other hand, the $\chi 4 =$ *trans* conformer gives an "elongated" structure. To describe the degree of bent of the chiral chain relative to the core moiety, we define a bent angle θ as $\cos\theta = \boldsymbol{a} \cdot \boldsymbol{b} / |\boldsymbol{a} \| \boldsymbol{b}|$ where $\boldsymbol{a} = \overrightarrow{\mathrm{C1C2}}$, $\boldsymbol{b} = \overrightarrow{\mathrm{C3C9}}$. This value is calculated to be 85° and 35° for the highly bent and elongated conformations, respectively. It is important to point out here that the NMR studies carried out in the SmA phase of MHPOBC [6,7] reported the value of 42–43°, which does not agree with either one of the above two values. This observation should indicate that the conformational transition takes place when the MHPOBC crystal melts into smectic phases. It is also important to note that the bent conformation found in the solid phase is not the most stable conformation but is the second stable conformation. Thus, if the packing constraints in the solid phase is removed, the more stable *trans* conformation and all other possible conformations are expected to be liberated. Unfortunately, however, neither MO nor NMR can directly analyze this conformational transition in connection with the change of molecular packing structure. In the next section, we therefore carry out

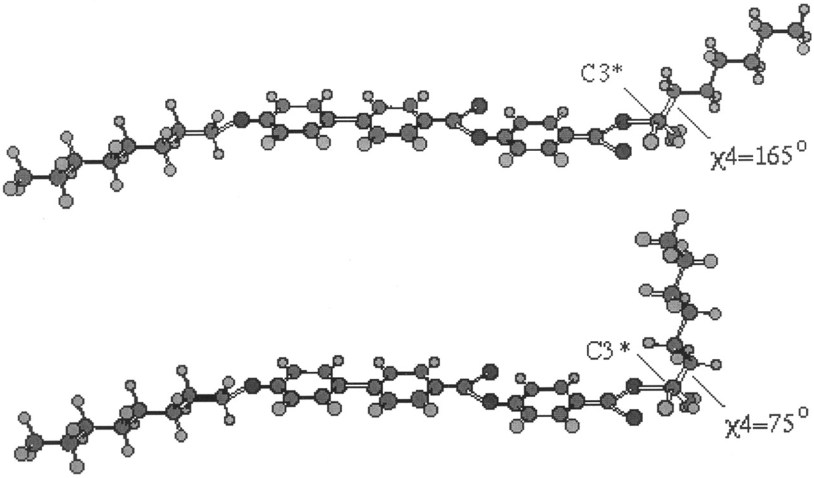

FIGURE 3 Calculated two major conformations of MHPOBC: (top) most stable conformation with ***trans*** χ4 (=165°) bond, bent angle $\theta = 35°$, (bottom) second stable conformation with ***gauche*** χ4 (=75°) bond, bent angle $\theta = 85°$.

molecular dynamics (MD) simulation and analyze the interplay of molecular conformational changes and packing structure transition in smectic phases.

(2) MD Simulation

Figure 4 shows a series of snapshots of the MHPOBC packing structure obtained from MD simulation (after 200 ps time evolution).

The simulation at 298 K (solid phase) reproduces the X ray structure, where the chiral alkyl chain is oriented nearly perpendicular to the core moiety. The mesogenic core group shows no significant thermal fluctuations: The core orientational correlation function $\langle P_2(\cos\theta_{ij})\rangle = \langle (3\cos^2\theta_{ij} - 1)/2\rangle$, where θ_{ij} is the angle between biphenyl axes (χB in Fig. 1) of molecules i and j, is calculated to be 1.0. The average orientation angle of the chiral chain relative to the core group is calculated to be $\theta = 71°$. This value is slightly smaller than the result of X-ray analysis (85°). A possible cause for this discrepancy may be found in the fact that the force parameters used in the present study are rather soft compared to other sets of parameters.

At 400 K, thermal motions of both core and end chains become more significant. The molecular packing structure seems not to be very much different from that in the solid phase at 298 K. However, when this structure is viewed along the long molecular axis Figure 5, it becomes clear that

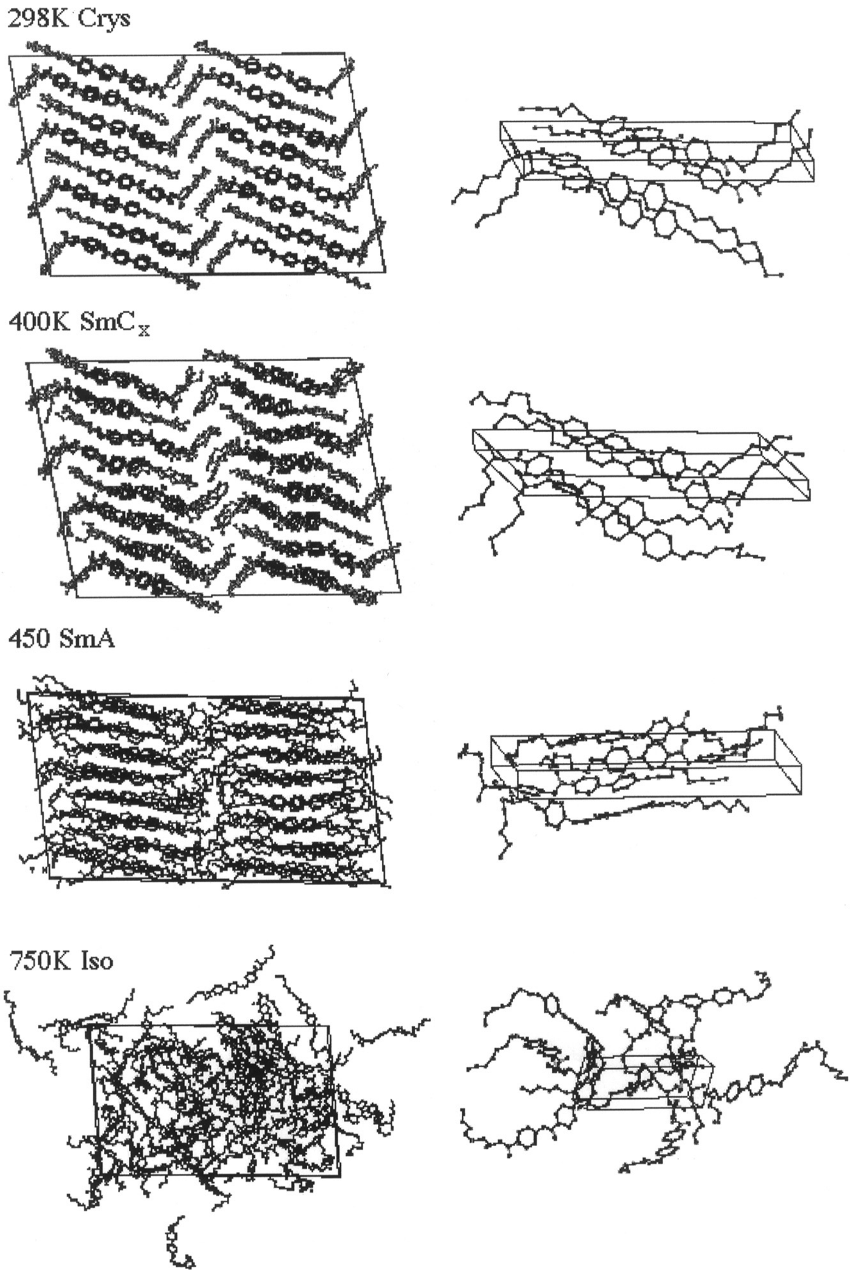

FIGURE 4 Snapshots of the molecular packing structure of MHPOBC calculated by MD simulation at (a) 298 K, (b) 400 K, (c) 450 K and (d) 750 K.

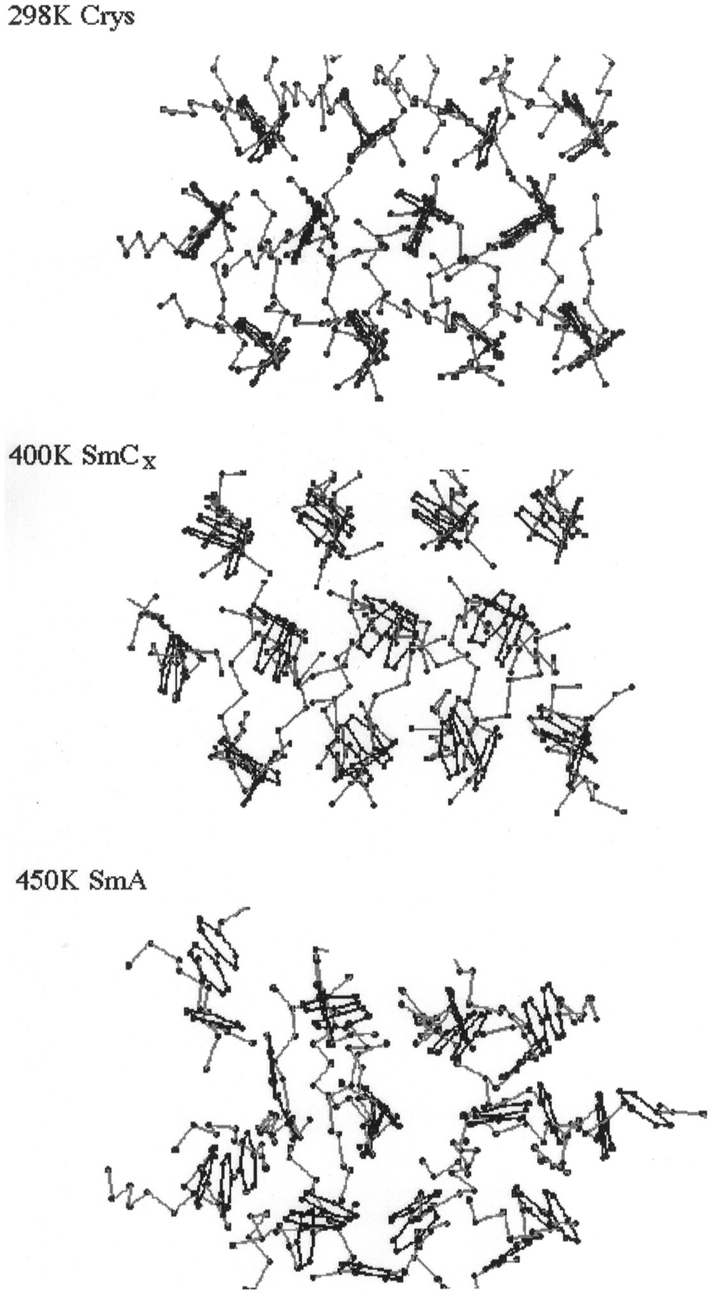

FIGURE 5 Snapshot of the MHPOBC packing structure viewed along the average orientation direction of the biphenyl core group at (a) 298 K, (b) 400 K and (c) 450 K.

the mosogen core (biphenyl group) in this phase is packed in an alternately tilted structure. This structure does not correspond to the "anti-clinic" structure in which the alternating tilt appears along the long molecular axis, nevertheless the structure at 400 K is clearly different from that in the crystalline phase at 298 K and hereafter this phase will be disignated as a SmC_x phase. The core orientational order parameter and the average bent angle θ are calculated to be 0.98 and 77°, respectively. This θ value indicates that the alkyl end-chain conformation starts melting in the SmC_x phase.

At 450 K (Fig. 4c), the tilted layer structure disappears. The molecules in this phase are uniaxially aligned along the layer direction: the degree of core orientational order is calculated to be 0.95. It is also evident that the alkyl chain conformation is liberated in this phase and the average molecular shape changes from the "highly bent" structure observed at low temperatures into a "moderately bent" or "elongated" structure. Thus, the 450 K structure is distinguished from the two previous low-temperature phases and is identified as a SmA phase.

The average molecular bent angle θ in this phase is calculated to be 46°. It should be emphasized that this value agrees quite well with the experimental value determined by ^{13}C-NMR (43°) and ^{2}H-NMR (42°) measurements. This bent angle (46°), however, does not correspond to either one of the two stable structures discussed in Figure 3 ($\theta = 85°$ or 35°). Obviously, this value is given as an average over a number of thermodynamically allowed conformations. In other words, there is no solid "moderately bent structure" in the SmA phase as opposed to the case of "highly bent structure" in the solid phase.

The simulation at 750 K generates an isotropic phase, where the MHPOBC molecules undergo free translational and rotational motion as well as internal bond rotation. The core orientational correlation function $\langle P_2(\cos\theta_{ij})\rangle$ in this phase is calculated to be zero.

Figure 5 shows the molecular packing structure in solid (298 K), SmC_x (400 K) and SmA (450 K) phases, viewed along the average orientation direction of the molecular principal axis (biphenyl *para*-axis). In the solid phase, all the principle axes of the molecules are aligned in one direction; both the biphenyl and phenyl groups can be seen only from their edges. In the SmC_x at 400 K, however, the biphenyl groups are no longer oriented in the same direction but are tilted toward mutually opposite directions from layer to layer. This packing structure distinguishes the 400 K phase from both the solid phase at 298 K and the SmA phase at 450 K. In the latter phase, the biphenyl groups are tilted in random directions and by random degrees. The positional order of the center of mass is also decreased.

Another evidence that supports the SmC_x phase formation can be found in the $\chi 4$ conformer distribution curve shown in Figure 6. As stated above,

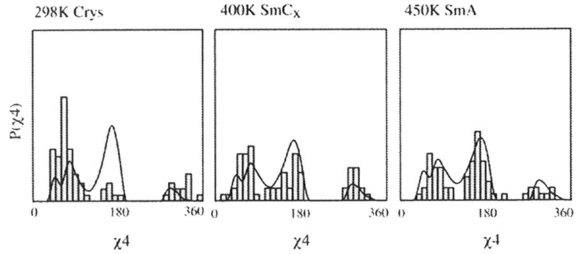

FIGURE 6 Rotamer distribution curves for the chiral chain $\chi 4$ (O1-C3*-C4-C5) bond at 298 K, 400 K and 450 K; histogram: MD simulation, solid curve: Boltzman distribution calculated by molecular orbital method.

the MO calculation (solid line) indicates that the *gauche* conformer at $\chi 4 = 300°$ is destabilized because of steric interactions between C5 (methylene) and C10 (methyl) groups (Fig. 2). Among other two possible conformers, the *trans* $\chi 4$ conformer (165°) is energetically more favored, however, the X-ray study has shown that MHPOBC in the crystalline phase assumes the *gauche* $\chi 4$ conformation (75°) that leads to the bent molecular structure. The result of MD simulation at 298 K (histogram in Fig. 6a) shows that the $\chi 4$ rotamer mainly concentrates in the *gauche* (75°) region in agreement with the X-ray observation. However, at 400 K (Fig. 6b), a considerable amount of the $\chi 4$ rotamer shifts from the *gauche* position to the *trans* position. The P($\chi 4$) distribution pattern at 400 K is clearly distingushable from that at 298 K and shows a close resemblance to the pattern at 450 K (Fig. 6c). At this latter temperature, the P($\chi 4$) distribution curve obtained from MD simulation shows a good agreement with the Boltzman distribution curve calculated for an isolated, single molecule by the MO method. It is also noteworthy that the torsion angle $\chi 4$ jumps between *trans* and two *gauche* states more than 10 times in 200 ps in the SmA phase. The comparison of the P($\chi 4$) curves at 400 K and 450 K clearly indicates that the conformation of the chiral alkyl chain (and of the achiral chain also) in these two phases is almost fully liberated into a fluid-like structure. Thus, from the conformational point of view, these two phases are distinguished from the solid phase at 298 K and are identified as smectic liquid crystalline phases. The 400 K and 450 K phases are then differentiated into SmC$_x$ (400 K) and SmA (450 K) phases from the molecular packing considerations as discussed in Figure 4.

CONCLUSION

In this paper we have shown that the MD simulation of MHPOBC can generate four distinct phases, *i.e.*, solid, SmC$_x$, SmA and isotropic phases.

In the solid phase, the MHPOBC molecule assumes a highly bent structure characterized by the ***gauche*** $\chi 4$ (= 75°) conformation. In the SmC_x phase, the molecules are packed in an alternately tilted molecular layer, and the $\chi 4$ bond has a larger population of the ***gauche*** (75°) conformer than the ***trans*** (165°) conformer. In the SmA phase, the $\chi 4$ conformation is almost fully liberated and the molecule assumes, on average, a moderately bent structure.

The MD simulation is so far the only technique that can visualize both molecular conformation and packing structure simultaneously. The fact that our MD simulation has been successful in generating the SmC_x and SmA phases for MHPOBC suggests that MD has a potential power to predict the existence of further complex smectic phases and analyze their structure for a family of MHPOBC and related compounds. We are aware of the fact that the present MD simulation does not exactly reproduce the actual phase-transition temperatures of MHPOBC. This is probably because of a size-effect, *i.e.*, we may need to increase the number of MHPOBC molecules to reproduce the thermodynamic properties associated with phase transition. Nevertheless, we believe that the molecular conformation in each phase, which is essentially determined by intramolecular interactions and short-range intermolecular constraints, can well be reproduced by the MD simulation. It is therefore still worth trying to perform several additional simulations at smaller temperature intervals to see the dynamic process of conformational melting during, for example, the SmC_x to SmA transition. If necessary, we will also examine the effect of the simulation cell size to check how much the phase transition temperature is influenced by the number of molecules considered. However, there is another important (probably more important than the above discussion on the size effect) extension of the present study. That is to calculate the ^{2}H-NMR quadrupolar splitting pattern observed for MHPOBC based on the results of our present MD simulation. If this is done, we can translate the experimental information obtained from ^{2}H-NMR (motionally averaged site-dependent bond orientational order parameters) into a distribution of discrete molecular conformers and thereby interpret the fundamental conformational property of antiferreoelctric liquid crystalline molecules with chiral alkyl endchains. Simulations along this direction are now being in progress and the results will be reported in future papers.

REFERENCES

[1] Chandani, A. D. L., Gorecka, E., Ouchi, Y., Takezoe, H., & Fukuda, A. (1989). *Jpn. J. Appl. Phys.*, *28*, L1265.

[2] Hori, K. & Endo, K. (1993). *Bull. Chem. Soc. Jpn.*, *66*, 46.

[3] Toriumi, H., Yoshida, M., Mikami, M., Takeuchi, M., & Mochizuki, A. (1996). *J. Phys. Chem.*, *100*, 15207.

[4] Seo, N. & Hori, K. (2001). *Liq. Cryst.*, *28*, 77.

[5] Yoshida, M., Seo, N., Hori, K., & Toriumi, H. (2001). *Mol. Crys. Liq. Crys.*, *365*, 813.

[6] Nakai, T., Miyajima, S., Takanishi, Y., Yoshida, S., & Fukuda, A. (1999). *J. Phys. Chem. B*, *103*, 406.

[7] Yoshida, S., Jin, B., Takanishi, Y., Tokumaru, K., Ishikawa, K., Takezoe, H., Fukuda, A., Kusumato, T., Nakai, T., & Miyajima, S. (1999). *J. Phys. Soc. Japan*, *68*, 9.

[8] Jin, B., Ling, Z., Takanishi, Y., Ishikawa, K., Takezoe, H., Fukuda, A., Kakimoto, M., & Kitazume, T. (1996). *Phys. Rev. E*, *53*, R4295.

[9] Stewart, J. J. (1989). *J. Comput. Chem.*, *10*, 209.

[10] Pople, J. A. & Beveridge, D. L. (1970). *Approximate Molecular Orbital Theory*, Mc-Graw-Hill.

[11] (a) Nose, S. (1984). *Mol. Phys.*, *52*, 255.
(b) Nose, S. (1984). *J. Chem. Phys.*, *81*, 511.

[12] (a) Parrinello, M. & Rahman, A. (1980). *Phys. Rev. Lett.*, *45*, 1196.
(b) Parrinello, M., & Rahman, A. (1981). *J. Appl. Phys.*, *52*, 7182.

[13] Mayo, S. L., Olafson, B.D., & Goddard, W. A. (1990). *J. Phys. Chem.*, *94*, 8897.

[14] Jorgensen, W. L. & Tirado-Rives, J. (1988). *J. Am. Chem. Soc.*, *110*, 1657.

[15] Ewald, P. P. (1921). *Ann. Phys.*, *64*, 253.